

The formation of nitro-aromatic compounds under high NO_x and anthropogenic VOC conditions in urban Beijing, China

Yujue Wang¹, Min Hu^{*,1,5}, Yuchen Wang³, Jing Zheng¹, Dongjie Shang¹, Yudong Yang¹, Ying Liu^{1,5}, Xiao Li¹, Rongzhi Tang¹, Wenfei Zhu⁶, Zhuofei Du¹, Yusheng Wu¹, Song Guo¹, Zhijun Wu¹, Shengrong Lou⁶, Mattias Hallquist², and Jian Zhen Yu^{*,3,4}

¹State Key Joint Laboratory of Environmental Simulation and Pollution Control, College of Environmental Sciences and Engineering, Peking University, Beijing 100871, China

²Department of Chemistry and Molecular Biology, University of Gothenburg, Gothenburg, Sweden

³Environmental Science Programs, Hong Kong University of Science & Technology, Hong Kong, China

⁴Department of Chemistry, Hong Kong University of Science & Technology, Hong Kong, China

⁵Beijing Innovation Center for Engineering Sciences and Advanced Technology, Peking University, Beijing 100871, China

⁶Shanghai Academy of Environmental Sciences, Shanghai 200233, China

Correspondence to: Min Hu (minhu@pku.edu.cn); Jian Zhen Yu (jian.yu@ust.hk)

Abstract. Nitro-aromatic compounds (NACs), as important contributors to the light absorption by brown carbon, have been widely observed in various ambient atmospheres, however, their formation in urban atmosphere was little studied. In this work, we report an intensive field study of NACs in summer 2016 at an urban Beijing site, characterized by both high-NO_x and anthropogenic VOCs dominated conditions. We investigated the factors that influence NAC formation (e.g. NO₂, VOC precursors, RH and photolysis) through quantification of 8 NACs, along with major components in fine particulate matter, selected volatile organic compounds and gases. The average total concentration of the quantified NACs was 6.63 ng/m³, higher than those reported in other summertime studies (0.14- 6.44 ng/m³). 4-Nitrophenol (4NP, 32.4%) and 4-nitrocatechol (4NC, 28.5%) were the top two most abundant NACs, followed by methyl-nitrocatechol (MNC), methyl-nitrophenol (MNP) and dimethyl-nitrophenol (DMNP). The oxidation of toluene and benzene in the presence of NO_x were found to be more dominant sources of NACs than primary biomass burning emissions. The NO₂ concentration level was found to be an important factor influencing the secondary formation of NACs. A transition from low- to high-NO_x regimes coincided with a shift from organic- to inorganic-dominated oxidation products. The transition thresholds were NO₂~20 ppb for daytime and NO₂~25 ppb for nighttime conditions. Under low-NO_x conditions, NACs increased with NO₂, while the NO₃⁻ concentrations and (NO₃⁻)/NACs ratios were lower, implying organic-dominated products. Under high-NO_x conditions, NAC concentrations did not further increase with NO₂, while the NO₃⁻ concentrations and (NO₃⁻)/NACs ratios showed increasing trends, signaling a shift from organic- to inorganic-dominated products. Nighttime enhancements were observed for 3M4NC and 4M5NC while daytime enhancements were noted for 4NP, 2M4NP and DMNP, indicating their different formation pathways for these two groups of NACs. Our analysis suggested that the aqueous-phase oxidation was likely the major formation pathways of 4M5NC and 3M5NC while photo-oxidation of toluene and benzene in the presence of NO₂ could be more

34 important for the formation of nitrophenol and its derivatives. Using the (3M4NC+ 4M5NC)/4NP ratios as an indicator of
35 the relative contribution of aqueous-phase and gas-phase oxidation pathways to NAC formation, we observed that the
36 relative contribution of aqueous-phase pathways increased at elevated ambient RH and remained constant at RH> 30%. We
37 also found that the concentrations of VOC precursors (e.g. toluene and benzene) and aerosol surface area acted as important
38 factors in promoting NAC formation, and photolysis as an important loss pathway for nitrophenols.

39

40 **1 Introduction**

41 Organic nitrogen, including nitro-aromatic compounds (NACs), N-heterocyclic compounds, amines and other organic
42 nitrate compounds containing (-NO₂) or (-NO₃) functional groups, represent an important fraction of ambient organic
43 aerosols (Laskin et al., 2009; Wang et al., 2017b; Chow et al., 2016; Ge et al., 2011; Ng et al., 2017). Among organic nitrogen,
44 NACs, with the -NO₂ and -OH functional groups attached to an aromatic ring, have gained much attention due to their light
45 absorbing property and impacts on human health (Mohr et al., 2013; Lin et al., 2017). NACs, including nitrophenols (NPs),
46 nitrocatechols (NCs) and their derivatives, are important contributors to the light absorption by brown carbon (BrC) (Mohr et
47 al., 2013; Teich et al., 2017; Zhang et al., 2013; Xie et al., 2017), contributing 50-80% of the total visible light absorption by
48 BrC emitted from biomass burning (Lin et al., 2017). Moreover, NACs also lead to mutagenesis and genotoxicity, thus
49 posing a threat to human health (Purohit and Basu, 2000; Huang et al., 1995).

50 NACs have been widely observed in various ambient atmospheres, including urban, suburban, rural, as well as
51 background environments, with the quantified concentrations varying from 0.1 ng/m³ in rural background areas to 147.4
52 ng/m³ in urban atmospheres (Iinuma et al., 2010; Teich et al., 2017; Zhang et al., 2010; Mohr et al., 2013; Chow et al., 2016;
53 Wang et al., 2018b). Combustion processes, especially biomass burning, were the most important primary sources of NACs
54 (Harrison et al., 2005; Wang et al., 2018b). The emission factors of NACs from biomass burning were estimated 0.8-11.1
55 mg/kg (Wang et al., 2017a; Hoffmann et al., 2007). Field observation studies indicated NACs are usually associated with
56 fresh or aged biomass burning aerosols, which contributed 10- 21% of the total NACs in ambient aerosols (Chow et al., 2016;
57 Kitanovski et al., 2012; Mohr et al., 2013; Iinuma et al., 2010; Wang et al., 2018b). Apart from primary emissions from
58 biomass burning, NACs could also be formed via the oxidation of volatile organic compounds (VOCs) containing a benzene
59 ring (e.g. cresol, catechol, methylcatechol) released by biomass burning in smoke plumes (Iinuma et al., 2010; Claeys et al.,
60 2012). Methyl-nitrocatechols (MNCs) could originate from NO_x oxidation of methylated cresol or methylcatechols, which
61 are released during biomass burning as thermal degradation products of lignin (Iinuma et al., 2010; Finewax et al., 2018;
62 Olariu et al., 2002). 4-Nitrocatechol could be formed via the OH-initiated oxidation of guaiacol, an abundant methoxyphenol
63 emitted from biomass burning, in the presence of NO₂ (Lauraguais et al., 2014). However, under high-NO_x conditions, this
64 pathway seems to be of minor importance to nitrocatechol formation, instead, nitroguaiacols were formed as the major

65 products (Lauraguais et al., 2014).

66 In urban atmosphere, aromatic VOCs such as benzene, toluene, and xylenes are expected to be important precursors to
67 NAC formation (Harrison et al., 2005). The main reactions leading to the secondary formation of NPs, NCs,
68 methyl-nitrophenols (MNPs) and MNCs are shown in Figure 1 (Jenkin et al., 2003; Vione et al., 2001; Vione et al., 2004;
69 Vidovic et al., 2018). Nitrophenols and its derivatives (e.g. MNPs) could originate through gas-phase oxidation of phenol,
70 benzene and toluene by OH or NO₃ radicals in the presence of NO₂ (Harrison et al., 2005; Yuan et al., 2016; Sato et al., 2007;
71 Ji et al., 2017; Olariu et al., 2002). Nitrocatechols dominated the composition of NACs formed in benzene/NO_x system (Xie
72 et al., 2017). The NC formation could be initiated by OH or NO₃ radicals to form β -hydroxyphenoxy/*o*-semiquinone radicals,
73 which then react with NO₂ to form the final products (Finewax et al., 2018). Compared with the gas-phase formation of
74 NACs, the formation pathway via aqueous-phase aromatic nitration is less well understood (Kroflc et al., 2018).
75 Nitrophenols could be formed through the hydroxylation and nitration of benzene in the presence of nitrite/nitrous acid or
76 photo-nitration of phenol upon UV irradiation of nitrite in aqueous solutions (Vione et al., 2004; Vione et al., 2001). It has
77 been suggested that nighttime aqueous-phase oxidation is an important formation pathway for methyl-nitrocatechols,
78 especially in polluted high-NO_x environments and in presence of acidic particles (pH around 3) (Vidovic et al., 2018). The
79 proposed aqueous-phase formation processes of MNCs include electrophilic substitution route and consecutive oxidation and
80 conjugated addition route (Frka et al., 2016; Vidovic et al., 2018). The loss pathways for NACs is proposed to include
81 photolysis and reactions with OH, NO₃ radicals or chlorine atoms (Atkinson et al., 1992; Bejan et al., 2007; Bejan et al.,
82 2015; Chen et al., 2011; Yuan et al., 2016; Hems and Abbatt, 2018).

83 However, few observational field studies have been conducted to investigate the formation of NACs in urban
84 atmospheres. In this work, we report results from an intensive field campaign conducted in summertime Beijing, aiming to
85 gain understanding of ambient concentration variation characteristics of NAC, relative importance of various proposed
86 formation pathways and major influence factors in high NO_x and anthropogenic VOCs dominated urban atmospheres. A
87 group of 8 NACs (NPs, MNPs, dimethyl-nitrophenols, DMNPs, NCs and MNCs) in 19 day samples and 19 night samples
88 were quantified using high performance liquid chromatography- mass spectrometry (HPLC-MS). Additional data of
89 inorganic aerosol constituents, VOC precursors, inorganic gases and meteorological parameters were also obtained and
90 analyzed to aid the investigation of the secondary formation pathways of NACs and controlling factors. This work provides
91 insights into the secondary formation of NACs in high NO_x and anthropogenic VOCs dominated urban environments.

92 2 Methods

93 2.1 Sample collection

94 As part of the bilateral Sweden-China framework research program on ‘Photochemical smog in China’, an intensive
95 field campaign was conducted in Beijing, aiming to improve the understanding on secondary chemistry during
96 photochemical smog events in China (Hallquist et al., 2016). The campaign was conducted at Changping (40.14° N, 116.11°
97 E), a regional site northeast of Beijing urban area, from May 15 to June 5, 2016. During this period, the site was influenced
98 by anthropogenic pollutants from Beijing urban areas and under high-NO_x conditions, as suggested by field measurement
99 evidence reported in previous publications related to this campaign (Tang et al., 2018; Wang et al., 2018a). During May 17-
100 June 5, the daily average concentrations of benzene, toluene and NO_x were 66-922 ppt, 47-1344 ppt and 4.0-32.3 ppb,
101 respectively.

102 Day and night ambient PM_{2.5} (particles with aerodynamic diameter less than 2.5 μm) samples were collected on
103 prebaked quartz fiber filters (Whatman Inc.) and Teflon filters (Whatman Inc.) using a high-volume sampler (TH-1000C,
104 Tianhong, China) and a 4-channel sampler (TH-16A, Tianhong, China). The sampling flow rates were 1.05 m³/min and 16.7
105 L/min, respectively. The daytime samples were collected from 8:30 to 17:30 LT (UTC+8) and the nighttime ones from 18:00
106 to 8:00 LT (UTC+8) the next morning. Field blank samples were collected by placing filters in the samplers with the pump
107 off for 30 min.

108 2.2 Quantification of NACs

109 An aliquot of 25 cm² was removed from each filter sample and extracted in ultrasonic bath three times using 3, 2 and 1
110 mL methanol containing 30 μL saturated EDTA solution in methanol-acetic acid consecutively, each time for 30 min. The
111 extracts were then filtered through a 0.25 μm polytetrafluoroethylene (PTFE) syringe filter (Pall Life Sciences), combined,
112 and evaporated to dryness under a gentle stream of high-purity nitrogen. The dried samples were re-dissolved in 50 μL
113 methanol/water (1:1) containing 100 ppb 4-nitrophenol-2,3,5,6-*d*₄ as internal standard. The solution was centrifuged and the
114 supernatant was used for analysis, using Agilent 1260 LC system (Palo Alto, CA) coupled to QTRAP 4500 (AB Sciex,
115 Toronto, Ontario, Canada) mass spectrometer. The LC-MS system was equipped with an electrospray ionization (ESI)
116 source operated in negative mode. More details of the extraction and optimized MS parameters have been described in our
117 previous study (Chow et al., 2016).

118 Chromatographic separation was performed on an Acquity UPLC HSS T3 column (2.1 mm×100 mm, 1.8 μm particle
119 size; Waters, USA) with a guard column (HSS T3, 1.8 μm). The column temperature was kept at 45 °C and the injection
120 volume was 5.0 μL. The mobile eluents were (A) water containing 0.1% acetic acid (v/v) and (B) methanol (v/v) containing
121 0.1% acetic acid at a flow rate of 0.19 mL/min. The gradient elution was set as follows: started with 1% B for 2.7 min;
122 increased to 54% B within 12.5 min and held for 1.0 min; then increased to 90% B within 7.5 min and held for 0.2 min; and

123 finally decreased to 1% B within 1.8 min and held for 17.3 min until the column was equilibrated. Chromatograms of NAC
124 standards and an ambient sample are shown in Figure S1.

125 The quantified NAC species are listed in Table 1. The NACs were identified and quantified using the $[M-H]^-$ ions in the
126 extracted ion chromatogram (EIC), using authentic standards or surrogates with the same molecular formula (Table 1). The
127 standards included: 4-nitrocatechol (4NC), 4-nitrophenol (4NP), 2-methyl-4-nitrophenol (2M4NP), 3-methyl-4-nitrophenol
128 (3M4NP) and 2,6-dimethyl-4-nitrophenol (2,6DM4NP) from Sigma–Aldrich (St. Louis, MO, USA);
129 4-methyl-5-nitrocatechol (4M5NC) from Santa Cruz Biotech (Dallas, TX, USA). The recoveries of the target NACs were
130 91-106%. 4M5NC was employed as a surrogate standard to quantify 3M5NC and 3M6NC. However, a recent study
131 suggested that no 3M6NC could be detected in ambient aerosols and the MNC isomer could be an incorrect assignment of
132 3M4NC as 3M6NC (Frka et al., 2016). We cannot exclude the possibility of MNC isomer as 3M4NC due to a lack of
133 authentic standards. Employing 4M5NC as a surrogate standard, the concentrations of 3M6NC could be obviously
134 underestimated due to its poor ionization under ESI condition compared with that of 4M5NC (Frka et al., 2016). The
135 concentration of dimethyl-nitrophenol (DMNP) was the sum of three isomers. 2,6DM4NP was identified based on its
136 retention time matching that of the authentic standard (Figure S1), while we cannot exclude the possibility of the other two
137 DMNP isomers as ethylnitrophenols or methoxylated isomers.

138 **2.3 Other online and offline measurements**

139 Other online and offline instruments were also employed to obtain related database, which has been introduced in
140 details in our previous paper (Wang et al., 2018c). In brief, a high resolution time-of-flight aerosol mass spectrometer (AMS)
141 was used to measure the chemical composition of PM_{10} (Zheng et al., 2017). The aerosol surface area was calculated based on
142 the measurements of particle number and size distribution by a scanning mobility particle sizer (SMPS, TSI 3936) and an
143 aerosol particle sizer (APS, TSI 3321) (Yue et al., 2009; Wang et al., 2018a). VOCs were measured by a
144 proton-transfer-reaction mass spectrometer (PTR-MS). Gaseous NH_3 was measured using a NH_3 analyzer (G2103, Picarro,
145 California, USA) (Huo et al., 2015). Meteorological parameters, including relative humidity (RH), temperature, wind
146 direction and wind speed (WS) were continuously monitored by a weather station (Met one Instrument Inc.) during the
147 whole campaign.

148 Organic carbon (OC) and element carbon (EC) were analyzed using thermal/optical carbon analyzer (Sunset
149 Laboratory). The organic matter (OM) concentration was calculated by multiplying OC by 1.6 (Turpin and Lim, 2001).
150 Water soluble inorganic ions were quantified by an ion chromatograph (IC, DIONEX, ICS2500/ICS2000) following
151 procedures described in Guo et al. (2010). Aerosol acidity and liquid water content (ALWC) was then calculated using the
152 ISORROPIA-II thermodynamic model. ISORROPIA-II was operated in forward mode, assuming the particles are
153 “metastable” (Hennigan et al., 2015; Weber et al., 2016; Guo et al., 2015). The input parameters included: ambient RH,

154 temperature, particle phase inorganic species (SO_4^{2-} , NO_3^- , Cl^- , NH_4^+ , K^+ , Na^+ , Ca^{2+} , Mg^{2+}), and gaseous NH_3 . More details
155 and validation of the thermodynamic calculations have been described in our previous paper (Wang et al., 2018c).

156 2.4 Estimation of the gas-phase NACs

157 The concentrations of gas-phase NACs were not measured in this study. They were calculated based on the measured
158 particle-phase NAC concentrations and equilibrium absorption partitioning theory (Pankow, 1994a, b; Pankow et al., 2001)
159 (Eqs. 1, 2):

$$160 \quad F_p = \left(1 + \frac{C^*}{C_{OA}}\right)^{-1} = \frac{c_p}{c_g + c_p} \quad (\text{Eq. 1})$$

161 where F_p is the fraction of NACs in the particle-phase. C_{OA} is the concentrations of organic aerosols (OA), calculated to be
162 OC multiplying by 1.6. c_g and c_p are the concentrations of NACs in gas phase and particle phase, respectively. C^* is the
163 effective saturation mass concentration ($\mu\text{g}/\text{m}^3$), and is calculated using Eq. 2:

$$164 \quad C^* = \frac{M10^6 \zeta P_v}{760RT} \quad (\text{Eq. 2})$$

165 where M is the molecular weight of NACs (g/mol). ζ is the activity coefficient of the species (assumed =1). R is the gas
166 constant (8.314 J/(mol K)), T is the temperature (K), and P_v (Pa) is the saturated pressure. P_v at the average temperature
167 during the campaign (296 K) is calculated using the multiphase system online property prediction tool developed by
168 University of Manchester (UManSysProp, <http://umansysprop.seaes.manchester.ac.uk>). The vapor pressures were estimated
169 using Nannoolal approach, and the boiling points were estimated using the Joback and Reid approach.

170 The estimated P_v , F_p and gas-phase concentrations of NACs are listed in Table S1. 4NP and methyl-nitrophenols
171 (2M4NP and 3M4NP) were predicted to be mainly in the gas phase ($F_p < 10\%$) while DMNP, 4NC and MNC (3M6NC,
172 3M5NC and 4M5NC) were mainly in the particle phase ($F_p > 60\%$). The gas-phase DMNP and MNC ($F_p > 95\%$) would not be
173 further discussed in this study. While the equilibrium model gives reasonable estimation of F_p and gas-phase concentrations
174 for nitrocatechols, it overestimates the vapor pressure of NPs by several orders of magnitude (Bannan et al., 2017). The
175 estimated F_p (0.83%) was obviously lower than the measured values for 4NP. For example, Cecinato et al. (2005) measured
176 F_p of 4NP and 3M4NP to be 82% and 78%, respectively in downtown Rome; Le Breton et al. (2018) reported F_p of
177 nitrophenol at ~17% using Chemical-Ionization Mass Spectrometer (CIMS) coupled with the Filter Inlet for Gases and
178 AEROSols (FIGAERO) during this campaign. We note that CIMS could not distinguish the isomers (e.g. 2NP) of 4NP,
179 however, the measured F_p values showed us the range of particulate fraction of 4NP during the campaign. The equilibrium
180 absorption partitioning model could underestimate the F_p of 4NP by ~20 times. Thus, the gas-phase 4NP concentration was
181 roughly calculated using the measured F_p (17%) by FIGAERO-CIMS (Le Breton et al., 2017).

182 Gas-phase NACs could also dissolve into the aqueous-phase particles. The concentrations dissolved into the aqueous
183 phase (C_{aq}) were estimated by Henry's law (Sander, 2015). Henry constants were obtained from Sander et al. (2015) and

184 ALWC was estimated using ISORROPIA-II (see section 2.4). The estimated C_{aq} of 4NP and 3M4NP were $4.4E-4$ and
185 $2.4E-5$ ng/m^3 , contributing $<0.02\%$ to their concentrations in particle phase. The contribution of dissolution into
186 aqueous-phase particles for NC and MNC is expected to be lower, due to the much lower gas-phase concentrations than that
187 of 4NP. For this reason, we will not further consider the dissolution of NACs into particle aqueous phase.

188 3 Results and Discussion

189 3.1 Concentration and composition of NACs

190 The average concentration of quantified NACs was 6.63 ng/m^3 , ranging from 1.27 to 17.70 ng/m^3 in summer in Beijing.
191 Figure 2 compares the total NAC concentrations across this and prior studies, and the individual NAC concentrations are
192 compared in Figure S2 and Table S2. The total NAC concentration in this work was higher than those measured in other
193 studies conducted in summer in mountain, rural or urban environments (Teich et al., 2017; Kitanovski et al., 2012; Kahnt et
194 al., 2013; Zhang et al., 2013; Chow et al., 2016; Wang et al., 2018b), and comparable to those reported in the studies in
195 summertime Wangdu, China (Teich et al., 2017; Wang et al., 2018b) (Figure 2). Most NAC species (NC, MNP and MNC),
196 except for DMNP and NP, also showed elevated concentrations in Changping, compared with those reported in other
197 summertime studies (Figure S2). Influenced by the outflow from urban Beijing air masses, the site was under typical
198 high- NO_x conditions (Wang et al., 2018a), implying abundant potential secondary formation of NACs during the observation
199 period. A recent study suggested that nocturnal biogenic VOCs (BVOCs) oxidation would transfer from low- to high- NO_x
200 regimes and nearly all the BVOCs would be oxidized by NO_3 radicals, at a $NO_x/BVOCs$ ratio higher than 1.4 (Edwards et al.,
201 2017). If we approximate the BVOC concentrations to be the sum of isoprene, MVK+MACR (methyl vinyl ketone and
202 methacrolein), and monoterpenes, the $NO_x/BVOC$ ratios were higher than 8 (nighttime ratios higher than 20) (Figure S3). If
203 we further consider the major anthropogenic VOCs (toluene, benzene), $NO_x/VOCs$ ratios were higher than 5 (nighttime
204 ratios higher than 10) (Figure S3). The high- NO_x conditions during the campaign were expected to facilitate the oxidation of
205 aromatic hydrocarbons and the subsequent secondary formation of NACs. Other emissions from biomass burning and coal
206 combustion were also observed to be contributors of organic aerosols during the campaign (Tang et al., 2018), and they
207 could also be the precursor sources of NACs. Biomass burning episodes occurred during Wangdu campaign, indicating NAC
208 emissions from biomass burning (Teich et al., 2017; Tham et al., 2016), which explain the high NAC levels in summer in
209 Wangdu. The NAC concentrations during summer (including this study) are generally lower than those during spring,
210 autumn or winter, which could be due to stronger contributions from combustion sources (e.g. biomass burning and coal
211 combustion) during spring, autumn or winter than those during summer (Chow et al., 2016; Wang et al., 2018b; Kitanovski
212 et al., 2012; Kahnt et al., 2013).

213 The NAC compositions are shown in the inserted pie chart in Figure S2. 4-Nitrophenol and 4-nitrocatechol were the

214 most abundant ones among all the quantified NAC species, accounting for 32.4 % and 28.5 % of the total quantified NACs,
215 followed by methyl-nitrocatechols (4M5NC, 3M5NC and 3M6NC, 16.2%), methyl-nitrophenol (2M4NP and 3M4NP, 15.6%)
216 and dimethyl-nitrophenol (8.3%) (Table 1). The contribution of NP and NC could be larger when considering both gas- and
217 particle-phases. The average concentration of 4NC in both gas- and particle-phases was estimated 2.2 ng/m³ using
218 equilibrium absorption partitioning model. The total concentration of 4NP (13 ng/m³) in both gas- and particle-phases was
219 approximated using the measured F_p (17%) by FIGAERO-CIMS (Le Breton et al., 2017). Nitrophenols and nitrocatechols
220 were generally reported among the most abundant NAC species in previous studies (Table S2 and the references therein).
221 Nitrophenols could be formed via the oxidation of anthropogenic VOCs (e.g. benzene) in the presence of NO₂ and
222 nitrocatechols were found to dominate the composition of NAC products formed in benzene/NO_x system in laboratory
223 studies (Xie et al., 2017; Harrison et al., 2005; Yuan et al., 2016; Sato et al., 2007; Ji et al., 2017; Olariu et al., 2002). Thus, it
224 is not a surprise to observe the high concentrations of nitrophenol and nitrocatechol in the typical high-NO_x and
225 anthropogenic VOCs dominated environments in summer in Beijing.

226 The contribution of NP among the total NACs at Changping was higher than that in summer in Hong Kong, while that
227 of MNC was lower (Table S2 and the inserted pie charts in Figure S2). This NAC composition difference between
228 Changping and Hong Kong may be a result of different formation pathways for NPs and MNC and different environmental
229 conditions at two sites. The gas-phase oxidation of aromatic hydrocarbons (e.g. phenol, benzene) in the presence of NO₂ is a
230 major source of NPs (Harrison et al., 2005; Yuan et al., 2016; Sato et al., 2007; Ji et al., 2017; Olariu et al., 2002), while
231 aqueous-phase oxidation represents the important formation pathway for atmospheric MNC (Frka et al., 2016; Vidovic et al.,
232 2018). The ambient RH in Hong Kong (>70%) was significantly higher than that in summer in Beijing (5-81%, 37% on
233 average), thus the relative contribution of aqueous-phase pathways could be more dominant in Hong Kong, promoting the
234 aqueous-phase formation of MNC. The influence of ambient RH on NAC formation will be further discussed in Section 3.4.
235 In comparison, more abundant gas-phase formation of nitrophenol was expected in summer in Beijing, under higher
236 anthropogenic VOCs, high NO_x and low RH conditions. In addition, the lower temperature in summer in Changping was
237 more favorable for the partitioning of nitrophenols from gas phase into particle phase.

238 3.2 Temporal variations and sources of NACs

239 Temporal variations of the total quantified NAC concentrations are shown in Figure 3, along with particulate organics,
240 nitrate, potassium ion, toluene, benzene, acetonitrile, wind speed and RH. During the field campaign, four pollution episodes
241 (episodes I, II, III, IV), marked by grey shading in Figure 3, were identified through observation of elevated organic aerosols.
242 Elevated NAC concentrations were observed during pollution episodes, coinciding with the increasing of toluene, benzene,
243 acetonitrile and potassium. The correlations between NACs and other chemical components are shown in Table S3. The
244 potassium ion was employed to indicate particulate emissions from biomass burning. As the biomass burning-derived

245 immediate VOC precursors to NACs were not detected in this study, acetonitrile was used to track the variations of VOCs
246 released by biomass burning. It was noticed that NACs showed stronger correlations with toluene ($r=0.70^{**}$), benzene
247 ($r=0.64^{**}$) or acetonitrile ($r=0.61^{**}$) than those with potassium ($r=0.49^{**}$). This appeared to suggest that the NO_x oxidation
248 of anthropogenic VOCs and precursor VOCs from biomass burning was a more important source of NACs than primary
249 biomass burning emission in summer in Beijing. A lower correlation between particulate NACs and EC (Table S3, $r=0.39^{**}$)
250 was also in agreement with the suggestion of the less importance of primary emissions to NACs during the campaign. We
251 note that only particulate NAC concentrations were used to do the correlation analysis. Two atmospheric processes, namely
252 photolysis and gas-to-particle partitioning, could influence the abundance of particle-phase NACs, especially for NP and
253 MNPs, since majority of them was expected to be in the gas phase (Table S1). As such, correlations of particle-phase NP and
254 MNPs with other species may less reliably reflect the underlying associations with the correlation species. As for the relative
255 importance of anthropogenic VOCs and biomass burning-derived VOCs, we do not have direct field measurement data for
256 the differentiation. However, previous studies suggested that the sources of anthropogenic VOCs in summer in Beijing were
257 dominated by vehicle emissions (>50%), with minor contributions from solvent evaporation and biomass burning (Wang et
258 al., 2014; Liu et al., 2008). Modelling studies incorporating emission inventories of the relevant VOC precursors could
259 address this issue and are suggested in future investigation of NAC sources. We note that biomass burning could often be of
260 an anthropogenic origin. Within this work, the term “anthropogenic VOCs” does not include VOCs from human-caused
261 biomass burning activities.

262 To further investigate the formation of NACs, we examined the time series and day-night variations of individual NAC
263 species (Figures 4, S4 and S5). Daytime enhancements of 4NP, 2M4NP and DMNP, nighttime enhancements of 3M4NC and
264 4M5NC were observed, and other NAC species didn't show discernible day-night variations (Figures 4, S4 and S5),
265 indicating different formation pathways among NAC species. Good inter-species correlations were observed among
266 nitrophenol and its derivatives (2M4NP, 3M4NP, DMNP, $r=0.56-0.88$), as well as among nitrocatechol and its derivatives
267 (3M6NC, 3M5NC, 4M5NC, $r=0.49-0.84$). This signaled that the formation and loss pathways as well as the influence factors
268 were likely similar within NP and NC groups. In comparison, the correlations of NACs across the two groups, i.e., between
269 nitrophenol derivatives (MNP, DMNP) and nitrocatechol derivatives (MNC, $r=0.05-0.45$), were lower (Table S3), suggesting
270 different formation pathways and influence factors. NC and its derivatives showed stronger correlations with toluene,
271 benzene, acetonitrile and K^+ , compared with NP and its derivatives (Table S3). This was more likely associated with the fact
272 that particle-phase NPs only account for a minor part of the atmospheric NP abundance due to the high vapor pressure of
273 NPs (Table S1). The abundance of particulate NP could largely depend on gas-to-particle partitioning, which is strongly
274 affected by temperature, as well as their gas-phase loss pathways (e.g. photolysis) (Bejan et al., 2007; Yuan et al., 2016;
275 Sangwan and Zhu, 2018). NC and MNC were mainly present in the particle phase (Table S1). The oxidation degradation
276 rates and photolysis of NC and MNC were therefore much lower. A recent laboratory study found that OH uptake by MNC

277 particles was suppressed by a factor of 4 at RH 15-30% in comparison with dry condition, as a result of competitive
278 co-adsorption of water molecules that occupied reactive sites (Slade and Knopf, 2014). During the campaign, the ambient
279 RH was 37%. Such an RH condition rendered that the OH uptake by particles was suppressed and therefore heterogeneous
280 oxidation of MNC was unlikely important.

281 Nighttime enhancements of 4M5NC and 3M5NC were observed during the whole observation period (Figure 4). A
282 strong correlation between 4M5NC and 3M5NC and their similar temporal variations likely indicated shared similarity in
283 their formation pathways. Previous studies suggested that aqueous-phase oxidation (including photooxidation and nighttime
284 oxidation) is an important formation pathway for atmospheric MNC, especially in polluted high-NO_x environments and
285 relatively acidic particles (pH around 3) (Vidovic et al., 2018; Frka et al., 2016). 4M5NC and 3M5NC showed relatively
286 stronger correlations with RH compared with other NAC species (Table S3), implying the importance of water in their
287 formation processes and the aqueous-phase pathway. During the campaign, the acidic particles (a pH in the range of 2.0-3.7)
288 and the high-NO_x conditions (Wang et al., 2018c; Wang et al., 2018a) provided suitable environments for the aqueous-phase
289 oxidation formation of MNC. The nighttime enhancements of 4M5NC and 3M5NC were more obvious during episode I than
290 those during episodes II-IV (nighttime/daytime concentrations at 1.9-3.1 vs. 0.9-1.5) (Figure 4), which suggested that
291 nighttime aqueous-phase formation pathways played more important roles during the first episode. The daytime correlations
292 between 4M5NC or 3M5NC and RH or NO₂ were stronger than the nighttime (Table S4). The aqueous-phase NO_x oxidation
293 could be more dependent on ambient RH and NO₂ levels during the daytime, due to the lower RH and NO₂ concentrations
294 than those at night (Figures 3, S3). MNCs also showed good correlations with acetonitrile and potassium, as MNCs could
295 also be formed via the oxidation of biomass burning-derived VOC precursors (e.g. cresol) (Inuma et al., 2010; Finewax et
296 al., 2018; Olariu et al., 2002). 3M6NC (or 3M4NC isomer) showed different temporal variations from 4M5NC or 3M5NC
297 (Figures 4, S4) and their correlations were lower than that between 4M5NC and 3M5NC (Tables S3, S4), possibly
298 suggesting different formation pathway for 3M6NC (or 3M4NC isomer) from those of 4M5NC or 3M5NC. The quantum
299 calculations have predicted the formation of 3M5NC via aqueous-phase electrophilic substitution and nitration by NO₂⁺,
300 while the formation of 3M6NC was negligible due to higher activation barriers for nitration of 3-methylcatechol to form
301 3M6NC (Frka et al., 2016). A dominant presence of 3M5NC in ambient aerosols was also expected according to the
302 theoretical predictions (Frka et al., 2016). The 3M5NC concentration was higher than that of 3M6NC in summer in Beijing,
303 consistent with the suggestion from computation study by Frka et al (2016).

304 Different from the nighttime enhancements of 4M5NC and 3M5NC, 4NP, 2M4NP and DMNP showed daytime
305 enhancements during the whole campaign (Figures 4, S5). Previously, Yuan et al (2016) also suggested the daytime
306 gas-phase oxidation of aromatics could represent the major source of NPs, while the contribution from nighttime reaction of
307 phenol with NO₃ radicals was relatively lower (Yuan et al., 2016). The daytime enhancements of NP and its derivatives
308 (2M4NP, DMNP) were more prominent during episodes II-IV than episode I (daytime/nighttime concentrations at 3.1-4.5 vs.

1.8-2.0) (Figure 4), which indicated that gas-phase photochemical oxidation play more important roles during the later period of campaign. We did not find good correlation between 4NP and NO₂ when considering the whole campaign period (Table S3), while good correlations were observed when treating the daytime and nighttime conditions separately (Table S4). The strong correlations between 4NP and benzene, toluene or NO₂ during daytime and nighttime indicated its formation via oxidation of benzene and toluene in the presence of NO₂ (Table S4). The formation mechanisms of nitrophenol were different during daytime (OH-initiated photooxidation of aromatics in the presence of NO₂) and nighttime (NO₃⁻-initiated oxidation of aromatics) (Harrison et al., 2005; Yuan et al., 2016; Sato et al., 2007; Ji et al., 2017; Olariu et al., 2002), thus the role and influence of NO₂ on NAC formation were different. For DMNP, 2M4NP and 3M4NP, they also showed good correlations with benzene, toluene and NO₂ during daytime, but the correlations were absent at night. Instead, their correlations with RH were higher at night, implying the possible formation via aqueous-phase pathways.

3.3 The NO₂ control of NACs formation

The analysis in section 3.2 suggests that NO_x oxidation of anthropogenic VOC precursors represented the dominant sources of NACs in summer in Beijing. To further investigate the impacts of NO₂ on NAC secondary formation, we plot the concentrations of NACs, nitrate (NO₃⁻) and the NO₃⁻/NAC ratios as a function of NO₂ levels (Figure 5). The variation of (NO₃⁻)/NACs ratios was employed to illustrate the relative abundance of inorganic nitrate and oxidized organic nitrogen. The variation during daytime and nighttime were separately considered due to the different atmospheric conditions and oxidation mechanisms.

Generally, higher concentrations of NACs and nitrate were observed with elevated NO₂ concentration levels, in a nonlinear fashion (Figure 5). During the daytime, NACs increased with NO₂, and NO₃⁻ concentrations and (NO₃⁻)/NACs ratios were lower at low-NO_x conditions (NO₂< 20ppb). As NO₂ increased to higher than 20 ppb, NAC concentrations did not increase with NO₂ any more, signaling the transition from NO_x-sensitive to NO_x-saturated regimes for NAC secondary formation. At the same time, the NO₃⁻ concentrations and (NO₃⁻)/NACs ratios showed increasing trends compared with those under low-NO_x conditions (NO₂< 20ppb) (Figure 5a, b, c). It was likely that the daytime NO₂ was in excess for the oxidation of ambient VOCs and the NAC formation at NO₂> 20 ppb. Then the excess NO₂ would be oxidized to form inorganic nitrate, producing a shift of products from organic- to inorganic-dominated conditions. Similarly, during nighttime a transition was observed at NO₂ ~25 ppb in which oxidation products were shifted from organic- to inorganic-dominance (Figure 5d, e, f). At NO₂> 25 ppb, the nighttime NAC formation became independent of NO₂ concentrations and inorganic nitrate dominated the NO_x oxidation products. The simplified mechanisms and schematic diagram of the competing formation of inorganic nitrates and NACs are shown in Figure S6. The nighttime NO₂ transition value (~25 ppb) was higher than the daytime one (~20 ppb). The higher anthropogenic VOC precursors (Figure S3) and different oxidation mechanisms (Figure 1) were the potential reasons for elevated NO₂ transition value at night.

340 The compositional variation of inorganic nitrate and NACs described in this work serves as an example in illustrating
341 that the transition from low- to high-NO_x regimes and the corresponding oxidation products shifting from organic- to
342 inorganic-dominated conditions existed in polluted urban atmospheres that are characterized by high NO_x and anthropogenic
343 VOCs. However, the mechanisms as well as transition thresholds were less understood compared with the well-known
344 BVOCs/NO_x atmospheres. More comprehensive investigation in urban atmospheres is needed to develop more quantitative
345 understanding of the NO_x regime transition. As only a limited number of VOC species were measured in this study, the NO_x
346 regime transition value was expressed by NO₂ concentrations rather than NO₂/VOC or NO_x/VOC ratios. We also note that
347 the NO_x regime transition values in other atmospheres could be quite different. The NO_x regime transition values deserve
348 further investigation through comprehensive lab simulation and field observations to seek a more robust parameter that can
349 be applied to various atmospheric environments.

350 The analysis in the previous section indicates that the formation pathways of different NAC species vary from each
351 other, thus the role and influence of NO₂ on their formation are different. The NAC compositions under similar NO₂
352 concentration levels were averaged, with a bin size of 10ppb NO₂. The variation of NAC compositions as a function of NO₂
353 levels is shown in Figure 6 to investigate the influence of NO₂ on NAC compositions. The contributions of NCs (standard
354 deviation < 12% within each NO₂ bin) increased and those of NPs (standard deviation < 12% within each NO₂ bin) decreased
355 at elevated NO₂ concentrations. The NAC composition remained relatively constant at NO₂ >20 ppb, which was
356 approximately the transition value from low- to high-NO_x regimes. The role of elevated NO₂ in promoting formation of NCs
357 was more obvious than that for NPs. The oxidation of aromatics (e.g. benzene, toluene and VOCs emitted from biomass
358 burning) in the presence of NO₂ represent the major formation pathway of NCs. The formation of NCs would increase with
359 the increasing of ambient NO₂. As particle-phase NP and MNP were strongly dependent on the gas-to-particle partitioning
360 and gas-phase loss (e.g. photolysis), their increasing trends as a function of NO₂ were not as obvious as those of NC and
361 MNC.

362 **3.4 Other influence factors on NACs formation**

363 Nitration of aromatic hydrocarbons (e.g. benzene and toluene) represents the major source of NACs in summer in
364 Beijing. NACs generally increased with the increasing of anthropogenic toluene and benzene (Figure 7). During daytime,
365 when toluene was higher than 0.6 ppb and benzene higher than 0.4 ppb, the NACs concentrations did not increase further
366 with VOC concentrations (Figure 7a, b). It was likely that toluene or benzene was in excess and the NAC formation became
367 independent of these precursors. Similarly, the nighttime formation of NACs would become insensitive to these precursors
368 when toluene was higher than 1 ppb and benzene higher than 0.6 ppb (Figure 7c, d). The transition values of toluene or
369 benzene was higher at night than those during the daytime. This could be due to the significantly higher NO₂ levels
370 (significant at p= 0.01 level) (Figure S3), with higher capacity to oxidize VOC precursors, and different oxidation

371 mechanisms at night.

372 Though the total NACs didn't show good correlations with ambient RH, good correlations between 3M4NC, 4M5NC
373 and RH were observed (Table S3, Figure 8). Nitrophenols and methyl-nitrophenols, dominated by gas-phase formation
374 pathways, were less affected by ambient RH. Aqueous-phase oxidation represented the major formation pathway of 3M4NC
375 and 4M5NC during the campaign, based on the analysis in section 3.2 and previous studies (Vidovic et al., 2018; Frka et al.,
376 2016). Elevated ambient RH would favor the water uptake of aerosols and decrease the aerosol viscosity, which favors the
377 uptake of organic precursors or other gas molecules into the particles, mass diffusion of reactants, and chemical reactions
378 within the particles (Vaden et al., 2011; Booth et al., 2014; Renbaum-Wolff et al., 2013; Shrestha et al., 2015; Zhang et al.,
379 2015), and thereby enhance the formation of 3M4NC and 4M5NC in aqueous phase.

380 The $(3M4NC + 4M5NC)/4NP$ mass concentration ratios were employed to indicate the relative contribution of
381 aqueous-phase and gas-phase pathways to NAC formation. The variations of $(3M4NC + 4M5NC)/4NP$ ratios as a function of
382 ambient RH during daytime and nighttime are shown in Figure 9. During daytime, this ratio increased with RH when
383 $RH < 30\%$, indicating elevated contribution of aqueous-phase pathways to NAC formation with higher RH conditions. The
384 ratio remained stable at $RH > 30\%$ during both daytime and nighttime, suggesting the relative contribution of aqueous-phase
385 and gas-phase pathways would not increase further with increasing RH beyond $RH > 30\%$ (Figures 9a and 9b). The ratio
386 during the nighttime was obviously higher than during the daytime, indicating that the aqueous-phase oxidation played more
387 important roles for NAC formation at night. The results implied the importance of aqueous-phase oxidation for the
388 secondary formation of oxidized organic nitrogen at elevated ambient RH. Due to the limited sample number obtained by
389 filter-based analysis in this study, the influence of RH or aerosol liquid water content on NAC formation needs further
390 confirmative investigation using controlled laboratory studies.

391 The NAC concentrations also showed good correlations with aerosol surface area (Figure 8b). Higher aerosol surface
392 area would facilitate the partitioning of gas-phase NAC products or precursors into particle phase and the aqueous-phase or
393 heterogeneous oxidation processes (Krofljic et al., 2015; Bauer et al., 2004; Fenter et al., 1996; Vidovic et al., 2018).
394 Photolysis is an important loss pathway of NACs and could be the dominant sink for nitrophenols in the gas phase (Bejan et
395 al., 2007; Yuan et al., 2016). The highest value of $J(O^1D)$ of each day was used to roughly represent the photolysis intensity.
396 The daytime NAC concentrations showed negative correlations with $J(O^1D)$ (Figure 8c, Table S4), suggesting photolysis as
397 an important sink for NACs during the daytime.

398

399 **4 Conclusions**

400 Nitroaromatic compounds (NACs) measurements from an intensive field campaign conducted in summer in Beijing

401 were examined to investigate the abundance and formation characteristics of NACs under high-NO_x and anthropogenic
402 VOCs dominated atmosphere. The average concentration of eight quantified NACs was 6.63 ng/m³, generally higher than
403 those reported in other summertime studies elsewhere. Among the eight NACs, 4-Nitrophenol (32.4%) and 4-nitrocatechol
404 (28.5%) were the most abundant, consistent with previous studies, and followed by methyl-nitrocatechol, methyl-nitrophenol
405 and dimethyl-nitrophenol.

406 Our analysis indicates that the secondary formation via oxidation of anthropogenic VOC precursors (e.g. toluene,
407 benzene) in the presence of NO₂ represented more important sources of NACs than primary biomass burning emissions in
408 summer in Beijing. We also observed a transition of oxidation products from organic- to inorganic-dominated conditions as
409 NO_x shifted from low- to high-NO_x regimes. The transition occurred at NO₂ of ~20 ppb for the daytime and ~25 ppb for the
410 nighttime atmosphere. Under low-NO_x conditions, NACs were observed to increase with NO₂, and the NO₃⁻ concentrations
411 and (NO₃⁻)/NACs ratios were lower. Under high-NO_x conditions, the NAC concentration did not further increase with NO₂
412 while the NO₃⁻ concentrations and (NO₃⁻)/NACs ratios would show increasing trends. The shift in relative abundance of
413 inorganic nitrate and NACs observed in this work serves as an example in illustrating the demarcation of the low- and
414 high-NO_x regimes in the anthropogenic VOCs-NO_x interacted conditions in polluted urban atmospheres and that NO₂ plays
415 important roles in the formation of NACs. The reaction mechanisms however are still unclear, which deserve further
416 laboratory and field investigation in future studies.

417 Different day-night variations were observed between the two sub-groups of NACs (i.e. nitrophenols and
418 nitrocatechols). Obvious nighttime enhancements of 3M4NC and 4M5NC, daytime enhancements of 4NP, 2M4NP and
419 DMNP were noted, indicating their different formation pathways. The aqueous-phase oxidation pathways are presumed to be
420 important for the formation of 4M5NC and 3M5NC, under the conditions with high NO_x concentrations and acidic particles
421 during the campaign. Photo-oxidation of toluene and benzene in the presence of NO₂ were more important for the formation
422 of nitrophenols. Subsequently, the (3M4NC+ 4M5NC)/4NP mass ratio was employed to probe the relative contribution of
423 aqueous-phase and gas-phase pathways to NAC formation. This ratio would initially increase with RH and remain relatively
424 consistent at RH > 30%, indicating elevated contribution of aqueous-phase pathways to NAC formation under higher RH
425 conditions. Aqueous-phase pathways played more important roles in NAC formation at night than those during the daytime.

426 VOC precursors, aerosol surface area and photolysis were also important factors influencing the NAC formation. NACs
427 generally increased with the increasing of toluene and benzene, implying nitration of aromatic hydrocarbons (e.g. benzene
428 and toluene) may represent the major secondary source of NACs in our study location. The NAC formation would become
429 independent of toluene and benzene, when the daytime concentrations were higher than 0.6 and 0.4 ppb, or the nighttime
430 ones higher than 1 and 0.6 ppb. In addition, aerosol surface area was also important factor promoting the NAC formation and
431 photolysis could be an important loss pathway of nitrophenols during the daytime.

432

433

434

435 *Data availability.* The data presented in this article are available from the authors upon request (minhu@pku.edu.cn).

436

437 **The Supplement related to this article is available online**

438

439 *Author contributions.* MiH, MaH, and SG organized the field campaign. YJW and YCW conducted the offline analysis and
440 analyzed the data. YJW wrote the manuscript with input from JY. All authors contributed to the measurements, discussing
441 results and commenting on the manuscript.

442

443 *Competing interests.* The authors declare that they have no conflict of interest.

444

445 *Acknowledgements.* This work was supported by National Natural Science Foundation of China (91544214, 91844301,
446 41421064, 51636003); National research program for key issues in air pollution control (DQGG0103); National Key
447 Research and Development Program of China (2016YFC0202000: Task 3); bilateral Sweden-China framework program on
448 ‘Photochemical smog in China: formation, transformation, impact and abatement strategies’ by the Swedish Research
449 council VR under contract (639-2013-6917).

450

451 **References:**

452 Atkinson, R., Aschmann, S. M., and Arey, J.: Reactions of hydroxyl and nitrogen trioxide radicals with phenol, cresols, and
453 2-nitrophenol at 296 ± 2 K, *Environ. Sci. Technol.*, 26, 1397-1403, 10.1021/es00031a018, 1992.

454 Bannan, T. J., Booth, A. M., Jones, B. T., O'Meara, S., Barley, M. H., Riipinen, I., Percival, C. J., and Topping, D.: Measured
455 Saturation Vapor Pressures of Phenolic and Nitro-aromatic Compounds, *Environ. Sci. Technol.*, 51, 3922-3928,
456 10.1021/acs.est.6b06364, 2017.

457 Bauer, S. E., Balkanski, Y., Schulz, M., Hauglustaine, D. A., and Dentener, F.: Global modeling of heterogeneous chemistry
458 on mineral aerosol surfaces: Influence on tropospheric ozone chemistry and comparison to observations, *J. Geophys. Res.*,
459 [Atmos.], 109, 10.1029/2003jd003868, 2004.

460 Bejan, I., Barnes, I., Olariu, R., Zhou, S., Wiesen, P., and Benter, T.: Investigations on the gas-phase photolysis and OH
461 radical kinetics of methyl-2-nitrophenols, *Phys. Chem. Chem. Phys.*, 9, 5686-5692, 10.1039/b709464g, 2007.

462 Bejan, I., Duncianu, M., Olariu, R., Barnes, I., Seakins, P. W., and Wiesen, P.: Kinetic study of the gas-phase reactions of
463 chlorine atoms with 2-chlorophenol, 2-nitrophenol, and four methyl-2-nitrophenol isomers, *J. Phys. Chem. A*, 119,
464 4735-4745, 10.1021/acs.jpca.5b02392, 2015.

465 Booth, A. M., Murphy, B., Riipinen, I., Percival, C. J., and Topping, D. O.: Connecting bulk viscosity measurements to
466 kinetic limitations on attaining equilibrium for a model aerosol composition, *Environ. Sci. Technol.*, 48, 9298-9305,
467 10.1021/es501705c, 2014.

468 Chen, J., Wenger, J. C., and Venables, D. S.: Near-ultraviolet absorption cross sections of nitrophenols and their potential
469 influence on tropospheric oxidation capacity, *J. Phys. Chem. A*, 115, 12235-12242, 10.1021/jp206929r, 2011.

470 Chow, K. S., Huang, X. H. H., and Yu, J. Z.: Quantification of nitroaromatic compounds in atmospheric fine particulate

471 matter in Hong Kong over 3 years: field measurement evidence for secondary formation derived from biomass burning
472 emissions, *Environ. Chem.*, 13, 665-673, 10.1071/en15174, 2016.

473 Claeys, M., Vermeylen, R., Yasmeeen, F., Gomez-Gonzalez, Y., Chi, X. G., Maenhaut, W., Meszaros, T., and Salma, I.:
474 Chemical characterisation of humic-like substances from urban, rural and tropical biomass burning environments using
475 liquid chromatography with UV/vis photodiode array detection and electrospray ionisation mass spectrometry, *Environ.*
476 *Chem.*, 9, 273-284, 10.1071/EN11163, 2012.

477 Fenter, F. F., Caloz, F., and Rossi, M. J.: Heterogeneous kinetics of N₂O₅ uptake on salt, with a systematic study of the role of
478 surface presentation (for N₂O₅ and HNO₃), *J. Phys. Chem.*, 100, 1008-1019, 10.1021/jp9503829, 1996.

479 Finewax, Z., de Gouw, J. A., and Ziemann, P. J.: Identification and quantification of 4-nitrocatechol formed from OH and
480 NO₃ radical-initiated reactions of catechol in air in the presence of NO_x: implications for secondary organic aerosol
481 formation from biomass burning, *Environ. Sci. Technol.*, 52, 1981-1989, 10.1021/acs.est.7b05864, 2018.

482 Frka, S., Sala, M., Kroflic, A., Hus, M., Cusak, A., and Grgic, I.: Quantum chemical calculations resolved identification of
483 methylnitrocatechols in atmospheric aerosols, *Environ. Sci. Technol.*, 50, 5526-5535, 10.1021/acs.est.6b00823, 2016.

484 Ge, X., Wexler, A. S., and Clegg, S. L.: Atmospheric amines – Part I. A review, *Atmos. Environ.*, 45, 524-546,
485 10.1016/j.atmosenv.2010.10.012, 2011.

486 Guo, H., Xu, L., Bougiatioti, A., Cerully, K. M., Capps, S. L., Hite, J. R., Carlton, A. G., Lee, S. H., Bergin, M. H., Ng, N. L.,
487 Nenes, A., and Weber, R. J.: Fine-particle water and pH in the southeastern United States, *Atmos. Chem. Phys.*, 15,
488 5211-5228, 10.5194/acp-15-5211-2015, 2015.

489 Hallquist, M., Munthe, J., Hu, M., Wang, T., Chan, C. K., Gao, J., Boman, J., Guo, S., Hallquist, A. M., Mellqvist, J.,
490 Moldanova, J., Pathak, R. K., Pettersson, J. B. C., Pleijel, H., Simpson, D., and Thynell, M.: Photochemical smog in China:
491 scientific challenges and implications for air-quality policies, *Natl. Sci. Rev.*, 3, 401-403, 10.1093/nsr/nww080, 2016.

492 Harrison, M. A. J., Barra, S., Borghesi, D., Vione, D., Arsene, C., and Iulian Olariu, R.: Nitrated phenols in the atmosphere: a
493 review, *Atmos. Environ.*, 39, 231-248, 10.1016/j.atmosenv.2004.09.044, 2005.

494 Hems, R. F., and Abbatt, J. P. D.: Aqueous Phase Photo-oxidation of Brown Carbon Nitrophenols: Reaction Kinetics,
495 Mechanism, and Evolution of Light Absorption, *ACS Earth and Space Chemistry*, 2, 225-234,
496 10.1021/acsearthspacechem.7b00123, 2018.

497 Hennigan, C. J., Izumi, J., Sullivan, A. P., Weber, R. J., and Nenes, A.: A critical evaluation of proxy methods used to
498 estimate the acidity of atmospheric particles, *Atmos. Chem. Phys.*, 15, 2775-2790, 10.5194/acp-15-2775-2015, 2015.

499 Hoffmann, D., Iinuma, Y., and Herrmann, H.: Development of a method for fast analysis of phenolic molecular markers in
500 biomass burning particles using high performance liquid chromatography/atmospheric pressure chemical ionisation mass
501 spectrometry, *J. Chromatogr. A*, 1143, 168-175, 10.1016/j.chroma.2007.01.035, 2007.

502 Huang, Q., Wang, L., and Han, S.: The genotoxicity of substituted nitrobenzenes and the quantitative structure-activity
503 relationship studies, *Chemosphere*, 30, 915-923, 10.1016/0045-6535(94)00450-9, 1995.

504 Huo, Q., Cai, X., Kang, L., Zhang, H., Song, Y., and Zhu, T.: Estimating ammonia emissions from a winter wheat cropland
505 in North China Plain with field experiments and inverse dispersion modeling, *Atmos. Environ.*, 104, 1-10,
506 10.1016/j.atmosenv.2015.01.003, 2015.

507 Iinuma, Y., Boge, O., Grafe, R., and Herrmann, H.: Methyl-nitrocatechols: atmospheric tracer compounds for biomass
508 burning secondary organic aerosols, *Environ. Sci. Technol.*, 44, 8453-8459, 10.1021/es102938a, 2010.

509 Jenkin, M. E., Saunders, S. M., Wagner, V., and Pilling, M. J.: Protocol for the development of the Master Chemical
510 Mechanism, MCM v3 (Part B): tropospheric degradation of aromatic volatile organic compounds, *Atmos. Chem. Phys.*, 3,
511 181-193, DOI 10.5194/acp-3-181-2003, 2003.

512 Ji, Y., Zhao, J., Terazono, H., Misawa, K., Levitt, N. P., Li, Y., Lin, Y., Peng, J., Wang, Y., Duan, L., Pan, B., Zhang, F., Feng,
513 X., An, T., Marrero-Ortiz, W., Secrest, J., Zhang, A. L., Shibuya, K., Molina, M. J., and Zhang, R.: Reassessing the
514 atmospheric oxidation mechanism of toluene, *Proc. Natl. Acad. Sci. USA*, 114, 8169-8174, 10.1073/pnas.1705463114, 2017.

515 Kahnt, A., Behrouzi, S., Vermeylen, R., Safi Shalamzari, M., Vercauteren, J., Roekens, E., Claeys, M., and Maenhaut, W.:
516 One-year study of nitro-organic compounds and their relation to wood burning in PM₁₀ aerosol from a rural site in Belgium,
517 *Atmos. Environ.*, 81, 561-568, 10.1016/j.atmosenv.2013.09.041, 2013.

518 Kitanovski, Z., Grgic, I., Vermeylen, R., Claeys, M., and Maenhaut, W.: Liquid chromatography tandem mass spectrometry

519 method for characterization of monoaromatic nitro-compounds in atmospheric particulate matter, *J. Chromatogr., A*, 1268,
520 35-43, 10.1016/j.chroma.2012.10.021, 2012.

521 Kroflic, A., Grilc, M., and Grgic, I.: Unraveling Pathways of Guaiacol Nitration in Atmospheric Waters: Nitrite, A Source of
522 Reactive Nitronium Ion in the Atmosphere, *Environ. Sci. Technol.*, 49, 9150-9158, 10.1021/acs.est.5b01811, 2015.

523 Kroflic, A., Hus, M., Grilc, M., and Grgic, I.: Underappreciated and Complex Role of Nitrous Acid in Aromatic Nitration
524 under Mild Environmental Conditions: The Case of Activated Methoxyphenols, *Environ. Sci. Technol.*,
525 10.1021/acs.est.8b01903, 2018.

526 Laskin, A., Smith, J. S., and Laskin, J.: Molecular characterization of nitrogen-containing organic compounds in biomass
527 burning aerosols using high-resolution mass spectrometry, *Environ. Sci. Technol.*, 43, 3764-3771, 10.1021/es803456n, 2009.

528 Lauraguais, A., Coeur-Tourneur, C., Cassez, A., Deboudt, K., Fourmentin, M., and Chođ, M.: Atmospheric reactivity of
529 hydroxyl radicals with guaiacol (2-methoxyphenol), a biomass burning emitted compound: Secondary organic aerosol
530 formation and gas-phase oxidation products, *Atmos. Environ.*, 86, 155-163, 10.1016/j.atmosenv.2013.11.074, 2014.

531 Le Breton, M., Wang, Y., Hallquist, Å. M., Pathak, R. K., Zheng, J., Yang, Y., Shang, D., Glasius, M., Bannan, T. J., Liu, Q.,
532 Chan, C. K., Percival, C. J., Zhu, W., Lou, S., Topping, D., Wang, Y., Yu, J., Lu, K., Guo, S., Hu, M., and Hallquist, M.:
533 Online gas and particle phase measurements of organosulfates, organosulfonates and nitrooxyorganosulfates in Beijing
534 utilizing a FIGAERO ToF-CIMS, *Atmos. Chem. Phys.*, 1-32, 10.5194/acp-2017-814, 2017.

535 Lin, P., Bluvshstein, N., Rudich, Y., Nizkorodov, S. A., Laskin, J., and Laskin, A.: Molecular chemistry of atmospheric brown
536 carbon inferred from a nationwide biomass burning event, *Environ. Sci. Technol.*, 51, 11561-11570, 10.1021/acs.est.7b02276,
537 2017.

538 Liu, Y., Shao, M., Fu, L., Lu, S., Zeng, L., and Tang, D.: Source profiles of volatile organic compounds (VOCs) measured in
539 China: Part I, *Atmos. Environ.*, 42, 6247-6260, 10.1016/j.atmosenv.2008.01.070, 2008.

540 Mohr, C., Lopez-Hilfiker, F. D., Zotter, P., Prevot, A. S., Xu, L., Ng, N. L., Herndon, S. C., Williams, L. R., Franklin, J. P.,
541 Zahniser, M. S., Worsnop, D. R., Knighton, W. B., Aiken, A. C., Gorkowski, K. J., Dubey, M. K., Allan, J. D., and Thornton,
542 J. A.: Contribution of nitrated phenols to wood burning brown carbon light absorption in Detling, United Kingdom during
543 winter time, *Environ. Sci. Technol.*, 47, 6316-6324, 10.1021/es400683v, 2013.

544 Ng, N. L., Brown, S. S., Archibald, A. T., Atlas, E., Cohen, R. C., Crowley, J. N., Day, D. A., Donahue, N. M., Fry, J. L.,
545 Fuchs, H., Griffin, R. J., Guzman, M. I., Herrmann, H., Hodzic, A., Iinuma, Y., Jimenez, J. L., Kiendler-Scharr, A., Lee, B.
546 H., Luecken, D. J., Mao, J., McLaren, R., Mutzel, A., Osthoff, H. D., Ouyang, B., Picquet-Varrault, B., Platt, U., Pye, H. O.
547 T., Rudich, Y., Schwantes, R. H., Shiraiwa, M., Stutz, J., Thornton, J. A., Tilgner, A., Williams, B. J., and Zaveri, R. A.:
548 Nitrate radicals and biogenic volatile organic compounds: oxidation, mechanisms, and organic aerosol, *Atmos. Chem. Phys.*,
549 17, 2103-2162, 10.5194/acp-17-2103-2017, 2017.

550 Olariu, R. I., Klotz, B., Barnes, I., Becker, K. H., and Mocanu, R.: FT-IR study of the ring-retaining products from the
551 reaction of OH radicals with phenol, o-, m- and p-cresol, *Atmos. Environ.*, 36, 3685-3697, 10.1016/S1352-2310(02)00202-9,
552 2002.

553 Pankow, J. F.: An absorption model of the gas/aerosol partitioning involved in the formation of secondary organic aerosol,
554 *Atmos. Environ.*, 28, 189-193, 10.1016/1352-2310(94)90094-9, 1994a.

555 Pankow, J. F.: An absorption model of gas/particle partitioning of organic compounds in the atmosphere, *Atmos. Environ.*, 28,
556 185-188, 10.1016/1352-2310(94)90093-0, 1994b.

557 Pankow, J. F., Seinfeld, J. H., Asher, W. E., and Erdakos, G. B.: Modeling the Formation of Secondary Organic Aerosol. 1.
558 Application of Theoretical Principles to Measurements Obtained in the α -Pinene/, β -Pinene/, Sabinene/, Δ 3-Carene/, and
559 Cyclohexene/Ozone Systems, *Environ. Sci. Technol.*, 35, 1164-1172, 10.1021/es001321d, 2001.

560 Purohit, V., and Basu, A. K.: Mutagenicity of nitroaromatic compounds, *Chem. Res. Toxicol.*, 13, 673-692,
561 10.1021/tx000002x, 2000.

562 Renbaum-Wolff, L., Grayson, J. W., Bateman, A. P., Kuwata, M., Sellier, M., Murray, B. J., Shilling, J. E., Martin, S. T., and
563 Bertram, A. K.: Viscosity of α -pinene secondary organic material and implications for particle growth and reactivity, *Proc.*
564 *Natl. Acad. Sci. USA*, 110, 8014-8019, 10.1073/pnas.1219548110, 2013.

565 Sander, R.: Compilation of Henry's law constants (version 4.0) for water as solvent, *Atmos. Chem. Phys.*, 15, 4399-4981,
566 10.5194/acp-15-4399-2015, 2015.

567 Sangwan, M., and Zhu, L.: Role of Methyl-2-nitrophenol Photolysis as a Potential Source of OH Radicals in the Polluted
568 Atmosphere: Implications from Laboratory Investigation, *J. Phys. Chem. A*, 122, 1861-1872, 10.1021/acs.jpca.7b11235,
569 2018.

570 Sato, K., Hatakeyama, S., and Imamura, T.: Secondary organic aerosol formation during the photooxidation of toluene: NOx
571 dependence of chemical composition, *J. Phys. Chem. A*, 111, 9796-9808, 10.1021/jp071419f, 2007.

572 Shrestha, M., Zhang, Y., Upshur, M. A., Liu, P., Blair, S. L., Wang, H. F., Nizkorodov, S. A., Thomson, R. J., Martin, S. T.,
573 and Geiger, F. M.: On surface order and disorder of alpha-pinene-derived secondary organic material, *J. Phys. Chem. A*, 119,
574 4609-4617, 10.1021/jp510780e, 2015.

575 Slade, J. H., and Knopf, D. A.: Multiphase OH oxidation kinetics of organic aerosol: The role of particle phase state and
576 relative humidity, *Geophys. Res. Lett.*, 41, 5297-5306, 10.1002/2014gl060582, 2014.

577 Tang, R., Wu, Z., Li, X., Wang, Y., Shang, D., Xiao, Y., Li, M., Zeng, L., Wu, Z., Hallquist, M., Hu, M., and Guo, S.: Primary
578 and secondary organic aerosols in summer 2016 in Beijing, *Atmos. Chem. Phys.*, 18, 4055-4068, 10.5194/acp-18-4055-2018,
579 2018.

580 Teich, M., van Pinxteren, D., Wang, M., Kecorius, S., Wang, Z., Müller, T., Močnik, G., and Herrmann, H.: Contributions of
581 nitrated aromatic compounds to the light absorption of water-soluble and particulate brown carbon in different atmospheric
582 environments in Germany and China, *Atmos. Chem. Phys.*, 17, 1653-1672, 10.5194/acp-17-1653-2017, 2017.

583 Tham, Y. J., Wang, Z., Li, Q., Yun, H., Wang, W., Wang, X., Xue, L., Lu, K., Ma, N., Bohn, B., Li, X., Kecorius, S., Größ, J.,
584 Shao, M., Wiedensohler, A., Zhang, Y., and Wang, T.: Significant concentrations of nitryl chloride sustained in the morning:
585 investigations of the causes and impacts on ozone production in a polluted region of northern China, *Atmos. Chem. Phys.*, 16,
586 14959-14977, 10.5194/acp-16-14959-2016, 2016.

587 Vaden, T. D., Imre, D., Beranek, J., Shrivastava, M., and Zelenyuk, A.: Evaporation kinetics and phase of laboratory and
588 ambient secondary organic aerosol, *Proc. Natl. Acad. Sci. USA*, 108, 2190-2195, 10.1073/pnas.1013391108, 2011.

589 Vidovic, K., Lasic Jurkovic, D., Sala, M., Kroflic, A., and Grgic, I.: Nighttime aqueous-phase formation of nitrocatechols in
590 the atmospheric condensed phase, *Environ. Sci. Technol.*, 52, 9722-9730, 10.1021/acs.est.8b01161, 2018.

591 Vione, D., Maurino, V., Minero, C., and Pelizzetti, E.: Phenol photonitration upon UV irradiation of nitrite in aqueous
592 solution I: effects of oxygen and 2-propanol, *Chemosphere*, 45, 893-902, 10.1016/s0045-6535(01)00035-2, 2001.

593 Vione, D., Maurino, V., Minero, C., Lucchiari, M., and Pelizzetti, E.: Nitration and hydroxylation of benzene in the presence
594 of nitrite/nitrous acid in aqueous solution, *Chemosphere*, 56, 1049-1059, 10.1016/j.chemosphere.2004.05.027, 2004.

595 Wang, H. C., Lu, K. D., Guo, S., Wu, Z. J., Shang, D. J., Tan, Z. F., Wang, Y. J., Le Breton, M., Lou, S. R., Tang, M. J., Wu,
596 Y. S., Zhu, W. F., Zheng, J., Zeng, L. M., Hallquist, M., Hu, M., and Zhang, Y. H.: Efficient N₂O₅ uptake and NO₃ oxidation
597 in the outflow of urban Beijing, *Atmos. Chem. Phys.*, 18, 9705-9721, 10.5194/acp-18-9705-2018, 2018a.

598 Wang, L., Wang, X., Gu, R., Wang, H., Yao, L., Wen, L., Zhu, F., Wang, W., Xue, L., Yang, L., Lu, K., Chen, J., Wang, T.,
599 Zhang, Y., and Wang, W.: Observations of fine particulate nitrated phenols in four sites in northern China: concentrations,
600 source apportionment, and secondary formation, *Atmos. Chem. Phys.*, 18, 4349-4359, 10.5194/acp-18-4349-2018, 2018b.

601 Wang, M., Shao, M., Chen, W., Yuan, B., Lu, S., Zhang, Q., Zeng, L., and Wang, Q.: A temporally and spatially resolved
602 validation of emission inventories by measurements of ambient volatile organic compounds in Beijing, China, *Atmos. Chem.*
603 *Phys.*, 14, 5871-5891, 10.5194/acp-14-5871-2014, 2014.

604 Wang, X., Gu, R., Wang, L., Xu, W., Zhang, Y., Chen, B., Li, W., Xue, L., Chen, J., and Wang, W.: Emissions of fine
605 particulate nitrated phenols from the burning of five common types of biomass, *Environ. Pollut.*, 230, 405-412,
606 10.1016/j.envpol.2017.06.072, 2017a.

607 Wang, Y., Hu, M., Lin, P., Guo, Q., Wu, Z., Li, M., Zeng, L., Song, Y., Zeng, L., Wu, Y., Guo, S., Huang, X., and He, L.:
608 Molecular characterization of nitrogen-containing organic compounds in humic-like substances emitted from straw residue
609 burning, *Environ. Sci. Technol.*, 51, 5951-5961, 10.1021/acs.est.7b00248, 2017b.

610 Wang, Y., Hu, M., Guo, S., Wang, Y., Zheng, J., Yang, Y., Zhu, W., Tang, R., Li, X., Liu, Y., Le Breton, M., Du, Z., Shang, D.,
611 Wu, Y., Wu, Z., Song, Y., Lou, S., Hallquist, M., and Yu, J.: The secondary formation of organosulfates under interactions
612 between biogenic emissions and anthropogenic pollutants in summer in Beijing, *Atmos. Chem. Phys.*, 18, 10693-10713,
613 10.5194/acp-18-10693-2018, 2018c.

614 Weber, R. J., Guo, H., Russell, A. G., and Nenes, A.: High aerosol acidity despite declining atmospheric sulfate

615 concentrations over the past 15 years, *Nature Geosci.*, 9, 282-285, 10.1038/ngeo2665, 2016.

616 Xie, M., Chen, X., Hays, M. D., Lewandowski, M., Offenberg, J., Kleindienst, T. E., and Holder, A. L.: Light absorption of
617 secondary organic aerosol: composition and contribution of nitroaromatic compounds, *Environ. Sci. Technol.*, 51,
618 11607-11616, 10.1021/acs.est.7b03263, 2017.

619 Yuan, B., Liggi, J., Wentzell, J., Li, S.-M., Stark, H., Roberts, J. M., Gilman, J., Lerner, B., Warneke, C., Li, R., Leithead, A.,
620 Osthoff, H. D., Wild, R., Brown, S. S., and de Gouw, J. A.: Secondary formation of nitrated phenols: insights from
621 observations during the Uintah Basin Winter Ozone Study (UBWOS) 2014, *Atmos. Chem. Phys.*, 16, 2139-2153,
622 10.5194/acp-16-2139-2016, 2016.

623 Yue, D., Hu, M., Wu, Z., Wang, Z., Guo, S., Wehner, B., Nowak, A., Achtert, P., Wiedensohler, A., Jung, J., Kim, Y. J., and
624 Liu, S.: Characteristics of aerosol size distributions and new particle formation in the summer in Beijing, *J. Geophys. Res.*,
625 114, 10.1029/2008jd010894, 2009.

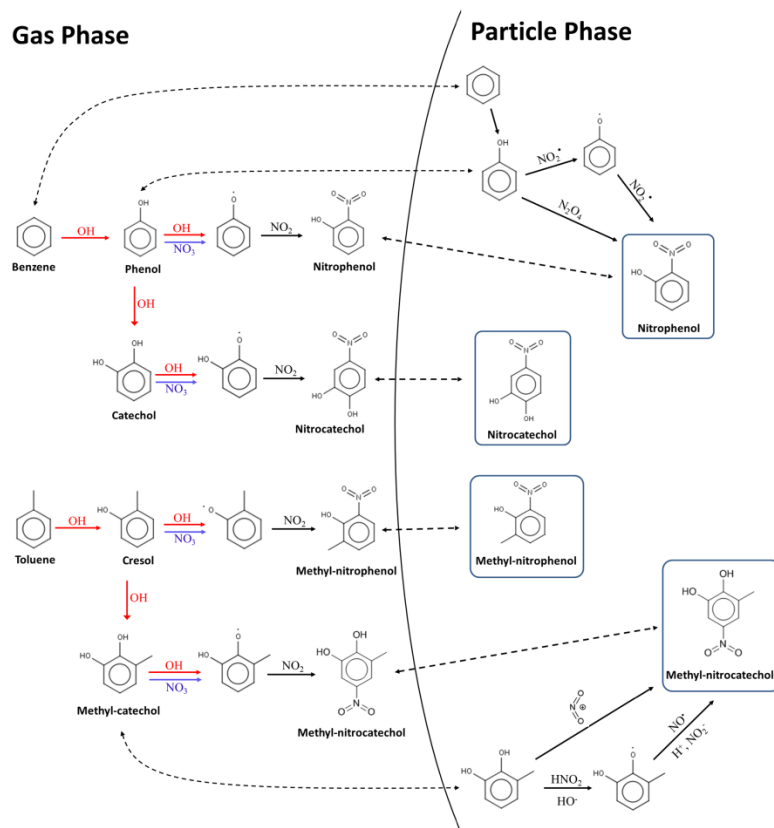
626 Zhang, X., Lin, Y. H., Surratt, J. D., and Weber, R. J.: Sources, composition and absorption Angstrom exponent of
627 light-absorbing organic components in aerosol extracts from the Los Angeles Basin, *Environ. Sci. Technol.*, 47, 3685-3693,
628 10.1021/es305047b, 2013.

629 Zhang, Y., Sanchez, M. S., Douet, C., Wang, Y., Bateman, A. P., Gong, Z., Kuwata, M., Renbaum-Wolff, L., Sato, B. B., Liu,
630 P. F., Bertram, A. K., Geiger, F. M., and Martin, S. T.: Changing shapes and implied viscosities of suspended submicron
631 particles, *Atmos. Chem. Phys.*, 15, 7819-7829, 10.5194/acp-15-7819-2015, 2015.

632 Zhang, Y. Y., Müller, L., Winterhalter, R., Moortgat, G. K., Hoffmann, T., and Pöschl, U.: Seasonal cycle and temperature
633 dependence of pinene oxidation products, dicarboxylic acids and nitrophenols in fine and coarse air particulate matter, *Atmos.*
634 *Chem. Phys.*, 10, 7859-7873, 10.5194/acp-10-7859-2010, 2010.

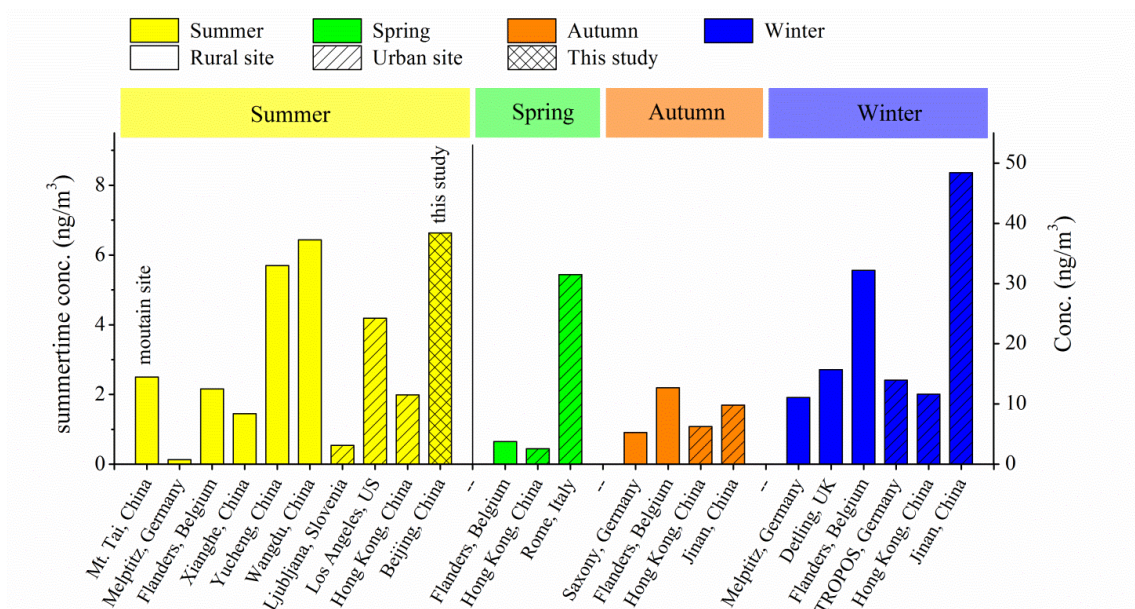
635 Zheng, J., Hu, M., Du, Z. F., Shang, D. J., Gong, Z. H., Qin, Y. H., Fang, J. Y., Gu, F. T., Li, M. R., Peng, J. F., Li, J., Zhang,
636 Y. Q., Huang, X. F., He, L. Y., Wu, Y. S., and Guo, S.: Influence of biomass burning from South Asia at a high-altitude
637 mountain receptor site in China, *Atmos. Chem. Phys.*, 17, 6853-6864, 10.5194/acp-17-6853-2017, 2017.

638



640

641 Figure 1 Schematic presentation of NAC secondary formation pathways via the oxidation of benzene, toluene, phenol and
 642 methycatechol in the gas phase and particle phase (Jenkin et al., 2003; Frka et al., 2016; Vione et al., 2004; Vione et al., 2001;
 643 Vidovic et al., 2018).

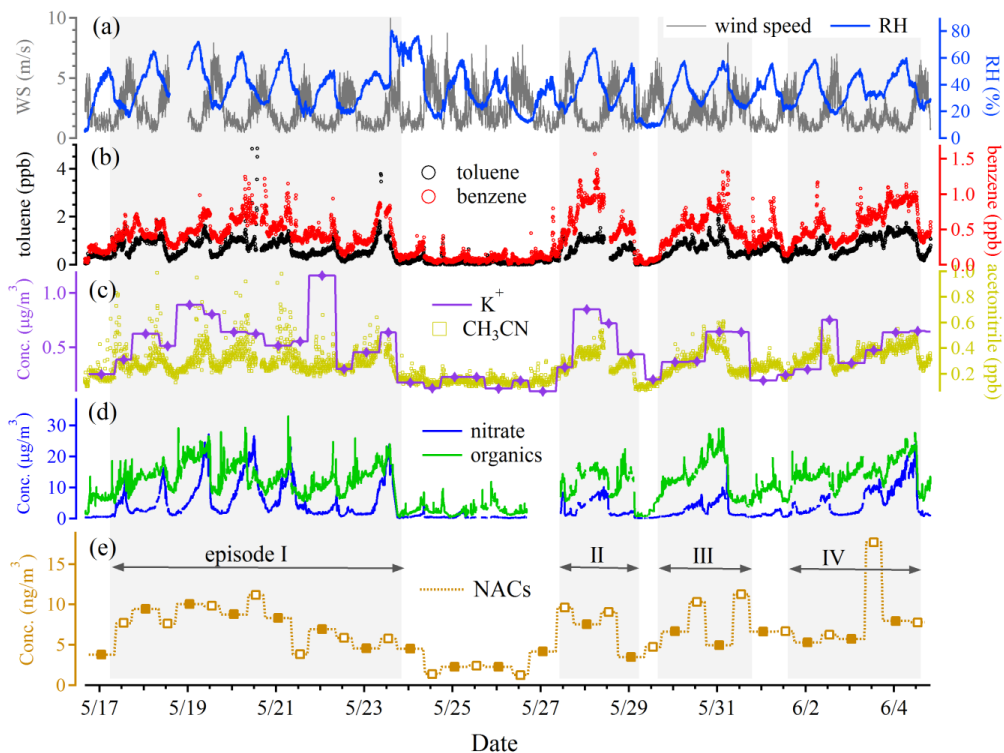


644

645 Figure 2 The summary of NAC concentrations cross this and prior studies (see Table S2 for the data and references therein).

646 The NAC concentrations in summer correspond to the left axis and other seasons correspond to the right axis.

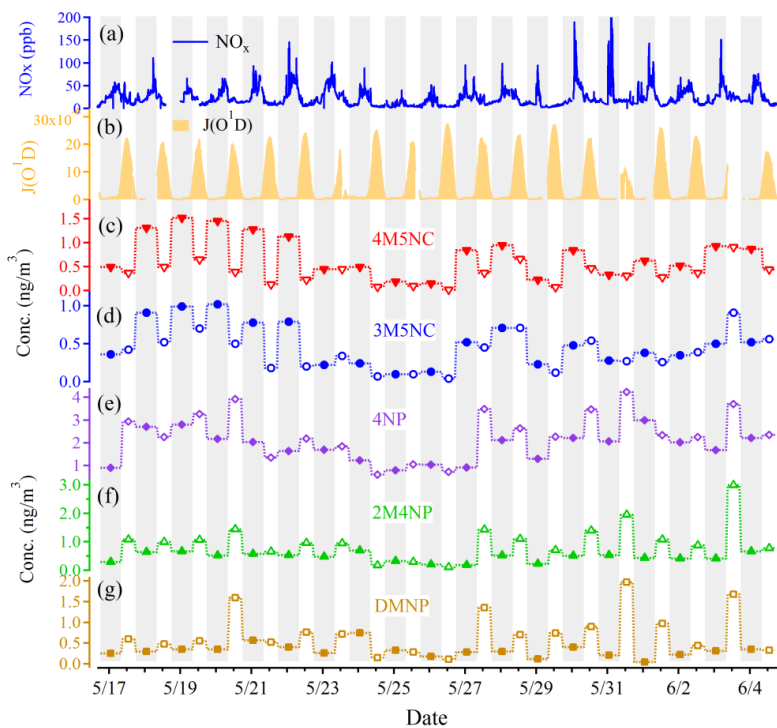
647



648

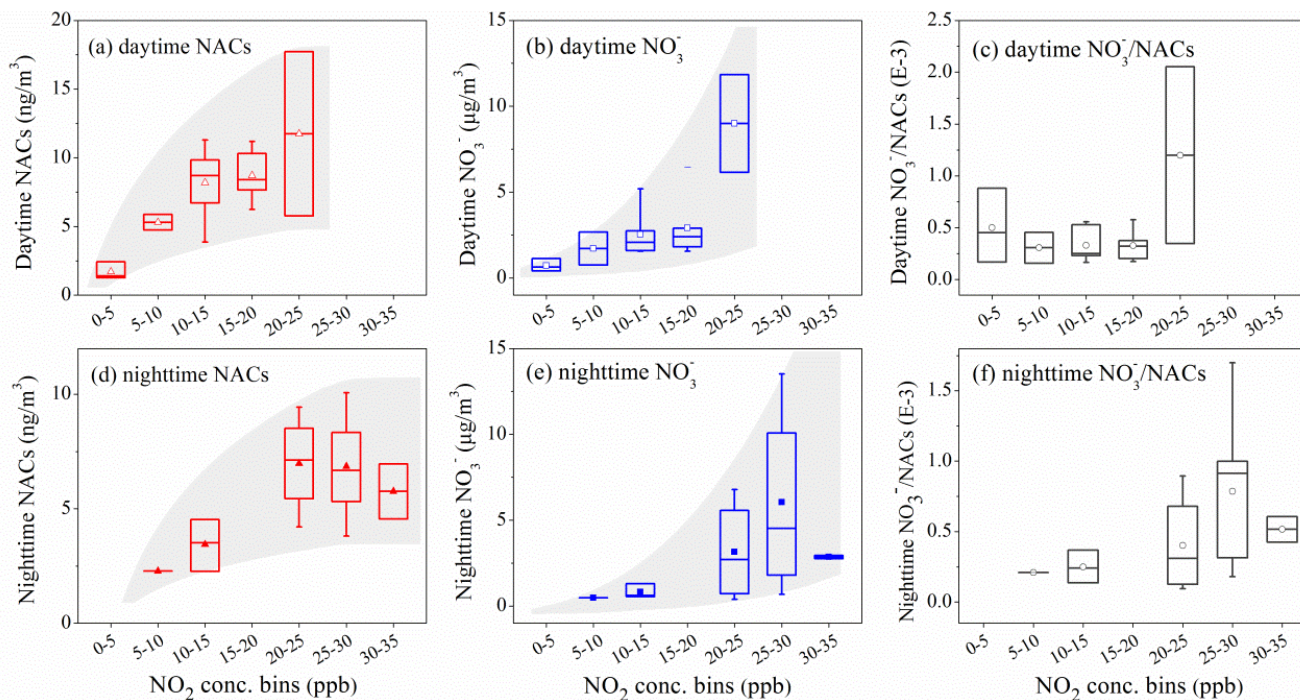
649 Figure 3 Time series of (a) wind speed (WS) and relative humidity (RH), (b) benzene and toluene, mass concentrations of (c)
 650 K^+ , (d) organics and nitrate, and (e) NACs. The pollution episodes, with elevated organic aerosols, are marked by gray
 651 shading.

652



653

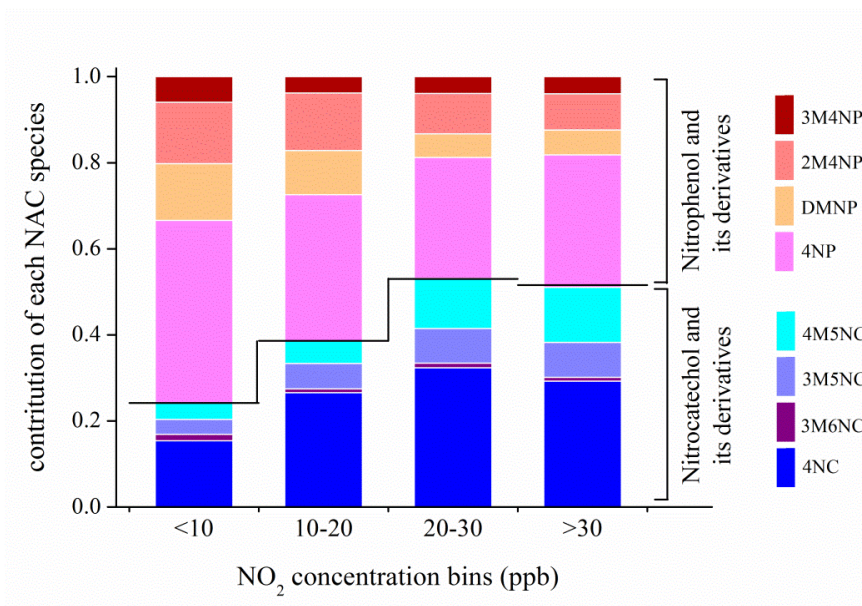
654 Figure 4 Time series of (a) NO_x , (b) $J(O^1D)$, (c) 4-methyl-5-nitrocatechol (4M5NC), (d) 4-methyl-5-nitrocatechol (3M5NC),
 655 (e) 4-nitrophenol (4NP), (f) 2-methyl-4-nitrophenol (2M4NP), and (g) dimethyl-nitrophenol (DMNP). The gray background
 656 denotes the nighttime and white background denotes the daytime.



658

659 Figure 5 The concentrations of NACs, nitrate and NO_3^-/NAC ratios as a function of NO_2 concentration bins during daytime
 660 and nighttime. The markers represent the mean values and whiskers represent 25 and 75 percentiles.

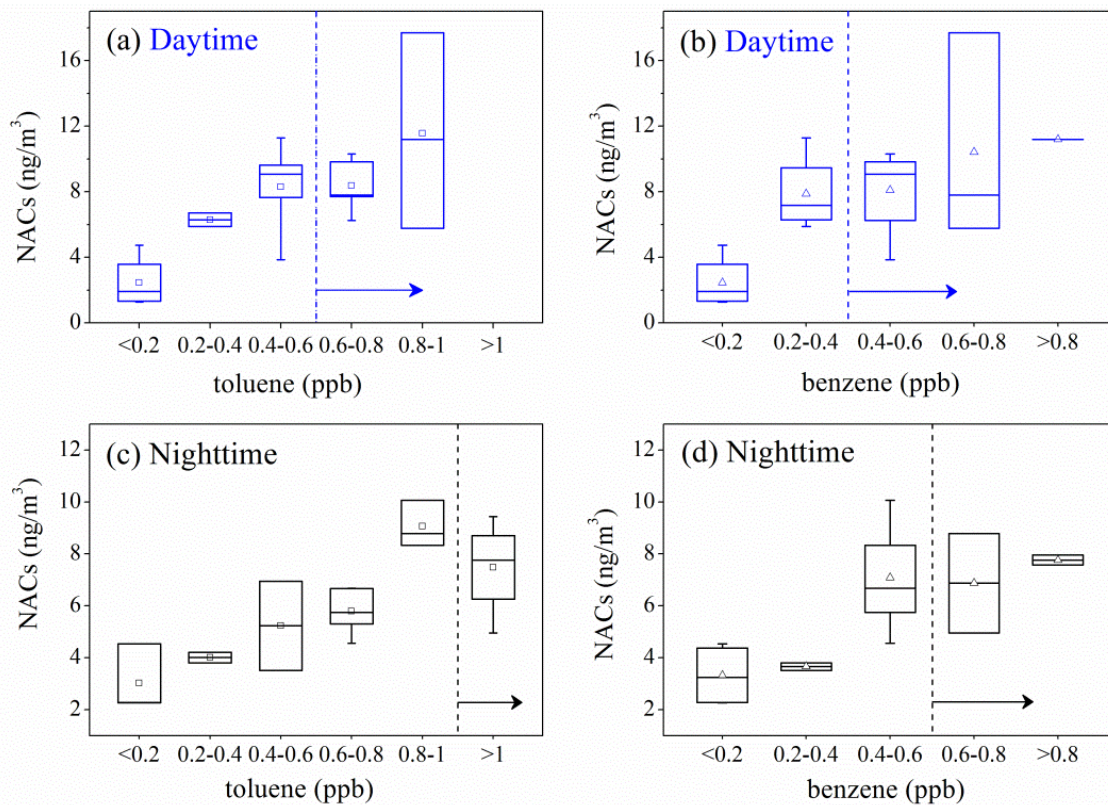
661



662

663 Figure 6 The variation of NAC compositions as a function of NO_2 concentration bins.

664



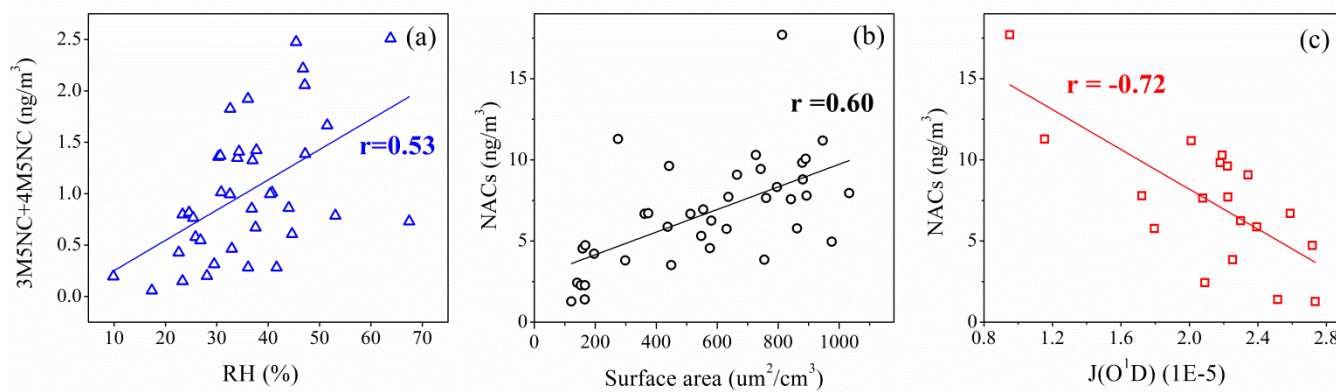
665

666 Figure 7 The concentrations of NACs as a function of toluene and benzene concentration bins during daytime and nighttime.

667 The markers represent the mean values and whiskers represent 25 and 75 percentiles.

668

669



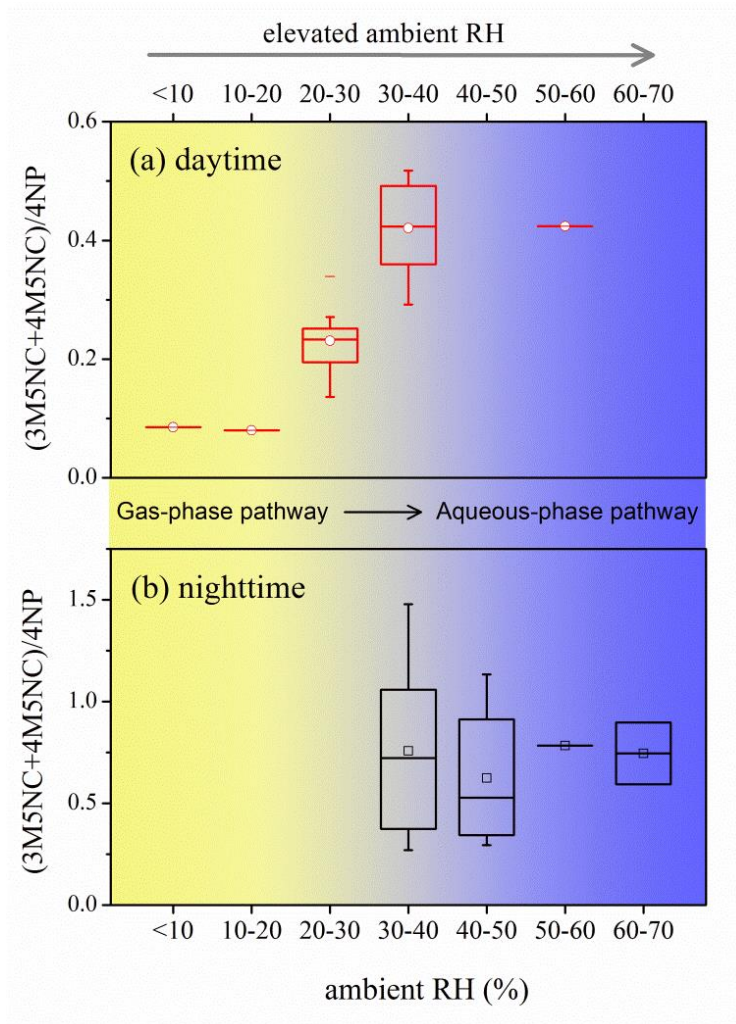
670

671 Figure 8 The correlation analysis (a) between (3M5NC+4M5NC) and RH, (b) between NACs and aerosol surface area,

672

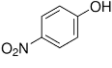
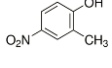
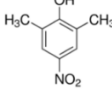
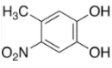
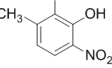
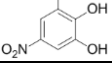
(c) between NACs and $J(O^1D)$.

673



674
 675 Figure 9 The $(3M5NC+4M5NC)/4NP$ concentration ratios as a function of ambient RH during (a) daytime and (b)
 676
 677
 678
 679
 680 nighttime.

Table 1 The quantified nitro-aromatic compounds in this study

compounds	formula	[M-H] ⁻	retention time (min)	standard	structure	range	average (n=38)
4NP	C ₆ H ₄ NO ₃ ⁻	138.02	21.3	4NP		0.60-4.24	2.15±0.93
3M4NP	C ₇ H ₆ NO ₃ ⁻	152.03	23.9	3M4NP		0.08-0.64	0.27±0.12
2M4NP	C ₇ H ₆ NO ₃ ⁻	152.03	24.9	2M4NP		0.11-2.99	0.76±0.55
DMNP	C ₈ H ₈ NO ₃ ⁻	166.05	26.0, 26.3, 26.9	2,6DM4NP		0.04-1.97	0.55±0.45
Total NP							3.72
4NC	C ₆ H ₄ NO ₄ ⁻	154.01	18.9	4NC		0.16-6.89	1.89±1.28
4M5NC	C ₇ H ₆ NO ₄ ⁻	168.03	21.8	4M5NC		0.02-1.52	0.56±0.40
3M6NC	C ₇ H ₆ NO ₄ ⁻	168.03	23.2	4M5NC		0.02-0.19	0.07±0.03
3M5NC	C ₇ H ₆ NO ₄ ⁻	168.03	23.5	4M5NC		0.04-1.02	0.44±0.27
Total NC							2.96